Conf-901116--40

UCRL-JC--105324

DE91 007260

Effects of Relativity of RTEX in Collisions of U^{q+} with Light Targets

M. H. Chen

This paper was prepared for the
Eleventh International Conference on the Application of
Accelerators in Research and Industry
Denton, TX
November 5-8, 1990

November 7, 1990

Lawrence Livermore National Laboratory

EFFECTS OF RELATIVITY ON RTEX IN COLLISIONS OF U^{q+} WITH LIGHT TARGETS

Mau Hsiung Chen

High Temperature Physics Division,
Lawrence Livermore National Laboratory
University of California
Livermore, CA 94550

We have calculated the resonant transfer and excitation cross sections in collisions of U^{q+} (q = 82, 89 and 90) ion with H_2, He and C in impulse approximation using the multi-configuration Dirac-Fock method. The calculations were carried out in intermediate coupling with configuration interaction. The quantum electrodynamic and finite nuclear size corrections were included in the calculations of transition energies. The Auger rates were calculated including the contributions from Coulomb as well as the transverse Breit interactions. For U^{89+} and U^{90+}, effects of relativity not only shift the peak positions but also change the peak structure. The total dielectronic recombination strength has been found to increase by 50% due to the effects of relativity. The present theoretical RTEX cross sections for U^{90+} in hydrogen agree well with experiment. For U^{82+}, Breit interaction has been found to have little effect on the RTEX cross sections involving L-shell excitation. However, the spin-orbit interaction can still make significant change in the peak structure.

I. INTRODUCTION

Excitation, ionization and charge transfer are the major atomic processes encountered in ion-atom collisions. For certain projectile energies, excitation of the ion and capture of a bound target electron can occur simultaneously in a single collision to form a resonant state of the projectile. This autoionizing state can subsequently decay by emitting either a photon (RTEX) or an Auger electron (RTEA) [1, 2]. In the past decade, intense experimental investigations [2-8] have been performed to study the RTEX process in ion-atom collisions. On the theoretical side, many calculations [9-16] based on the impulse approximation have been carried out. Most of these experimental and theoretical studies are concentrated on cases involving low- and mid-Z ions colliding with light targets. Recently, relativistic calculations for RTEX cross sections have been performed for U^{89+} and U^{90+} in collisions with light targets [13, 15]. Experimental investigations [7, 8] on these uranium ions have also been carried out to test the relativistic theory [13, 15]. In this paper, we will review the effects of relativity on the RTEX cross sections for U^{q+} (q = 82, 89 and 90) in collision with light targets (e.g. hydrogen, helium or carbon). The calculations were carried out in impulse approximation. The basic data such as energies and transition rates were evaluated by using the multiconfiguration Dirac-Fock [MCDF] model [17, 18].

II. CALCULATIONAL PROCEDURE

Resonant electron transfer and excitation in ion-atom collisions is an atomic process analogous to dielectronic recombination (DR) [19]. In a RTEX process, a weakly bound electron is captured instead of a free electron as in a DR event. Hence, the total RTEX cross section $\sigma^{X}_{RTE}(i)$ for an initial state i can be obtained in the impulse approximation by convoluting the DR cross section with the Compton profile of the target atom or molecule

$$\sigma^{x}_{RTE}(i) = \sum_{d} (M/2E)^{1/2} \, \Delta E \, \bar{\sigma}_{DR}(i \to d) J(Q) \quad , \tag{1}$$

with

$$Q = (E_d - Em/M)\,(M/2E)^{1/2} \tag{2}$$

Here, E is the projectile energy in the laboratory frame, M is the mass of the projectile, m is the electron mass, J(Q) is the Compton profile of the target atom or molecule, $\bar{\sigma}_{DR}(i \to d)$ is the energy-averaged DR cross section from state i to intermediate state d with energy bin ΔE, and E_d is the Auger energy in the rest frame of the ion.

In the isolated resonance approximation, the energy-averaged DR cross section $\bar{\sigma}_{DR}(i \to d)$ can be written in atomic units as

$$\bar{\sigma}_{DR}(i \to d) = \frac{\pi^2}{\Delta E \, E_d} \frac{g_d}{2g_i} \frac{A_a(d \to i) \sum_f A_r(d \to f)}{\sum_j A_a(d \to j) \sum_k A_r(d \to k)} \quad . \tag{3}$$

Here, g_d and g_i are the statistical weight factors for the states d and i, respectively; $A_a(d \to i)$ and $A_r(d \to k)$ are respectively the Auger and radiative rates.

In the present work, we only consider the correlated transfer excitation. The other uncorrelated transfer excitation processes [16] are not treated here.

For U^{89+} and U^{90+} ions in collisions with light targets, the resonant transfer and excitation followed by emission of a photon can be represented by

$$\begin{aligned} U^{89+}(1s^2 2s) + T &\to U^{88+}(1s2s\, n\ell\, n'\ell') + T^+ \\ &\hookrightarrow U^{88+}(1s^2 2s\, n''\ell'') + h\nu \quad , \end{aligned} \tag{4}$$

and

$$U^{90+}(1s^2) + T \rightarrow U^{89+}(1s\, n\ell\, n'\ell') + T^+$$
$$\hookrightarrow U^{89+}(1s^2\, n''\ell'') + h\nu \quad . \qquad (5)$$

In this work, we include the intermediate states from the $1s2s2\ell n\ell'$ ($2 \le n \le 12$ and $0 \le \ell' \le 3$) and $1s2s3\ell 3\ell'$ configurations for U^{89+}. In the case of U^{90+}, we include the contributions from the $1s2\ell n\ell'$ ($2 \le n \le 12$ and $0 \le \ell' \le 3$) configurations. For U^{82+}, we only consider the contributions from the L-shell excitation and capture to form the doubly-excited $3\ell 3\ell'$ configurations (i.e. $2s^22p^53\ell 3\ell'$ and $2s2p^63\ell 3\ell'$).

The detailed relativistic Auger and radiative transition rates are calculated from perturbation theory using the MCDF method [17, 18]. In the calculations of the relativistic Auger matrix elements, the two-electron operator is taken as a sum of the Coulomb and generalized Breit operators and can be expressed in atomic units by [20, 21]

$$V_{12} = \frac{1}{r_{12}} - \vec{\alpha}_1 \bullet \vec{\alpha}_2 \frac{\cos(\omega r_{12})}{r_{12}} + \left(\vec{\alpha}_1 \bullet \vec{\nabla}_1\right)\left(\vec{\alpha}_2 \bullet \vec{\nabla}_2\right)\frac{\cos(\omega r_{12}) - 1}{\omega^2 r_{12}} \quad , \qquad (6)$$

where $r_{12} = |\vec{r}_1 - \vec{r}_2|$ with $\vec{r}_1$ and $\vec{r}_2$ the position vectors; $\vec{\nabla}_1$ and $\vec{\nabla}_2$ are the gradient operators. The $\vec{\alpha}_i$ are the Dirac matrices and ω is the wave number of the exchanged virtual photon. The detailed information on the calculations of relativistic transition rates in the MCDF model has been presented in Ref. 18.

The atomic energy levels and bound-state wave functions were calculated using the MCDF model in the average-level scheme [17]. The calculations were carried out in intermediate coupling with configuration interaction from the same complex. The effects of transverse Breit interaction, quantum-electrodynamic corrections and finite nuclear size were included in the present work. All possible Auger channels and radiative electric-dipole transitions leading to stabilized bound states were accounted for in the evaluations of radiative branching ratios [Eq. (3)].

In order to study the effects of relativity on the RTEX cross sections, the calculations were repeated using the nonrelativistic limit of the MCDF model which can be achieved by increasing the velocity of light a thousand fold [17]. Furthermore, the Auger rates were calculated using two-electron operator [Eq. (6)] both with and without Breit interaction.

In the present work, Compton profiles for hydrogen molecule and helium were taken from experiment [22]. For the carbon target, theoretical Compton profiles [23] were employed.

III. RESULTS AND DISCUSSION

The effects of relativity on atomic transition probabilities can arise from several different factors: (1) changes in energies, (2) shifts in orbital wave functions, (3) relativistic aspects of the pertinent operators, viz, the magnetic interaction and retardation correction in the two-electron operator. The net effect on transition rates depends on the strength and relative phase of these factors. Relativistic calculation of x-ray and Auger transition probabilities has been reviewed recently [24].

For U^{88+} and U^{89+}, relativity increases the K-LL Auger energies by 2-18 KeV and can change some of the individual transition rates by orders of magnitude (e.g. the Auger rate for the $1s2s(0)\ 2p_{1/2}\ J = 1/2$ state of U^{89+} is increased by a factor of 100 due to relativity). In the RTEX calculations, the effects of relativity are partly washed out by the convolution of the DR cross sections with the Compton profiles of the target. For the $U^{89+} + H_2$ collisions, there is only one RTEX peak for the K-LL DR capture in the nonrelativistic LS coupling approximation. The effects of relativity and spin-orbit interaction shift the K-LL peak to higher energy and split it into three peaks. The total DR resonance strength is increased by 50% due to the effects of relativity [13]. Similar relativistic effects have also been found for the U^{90+} ion.

In Fig. 1, the RTEX cross sections for U^{89+} + H_2 system from the MCDF calculations with and without Breit interaction in the Auger operator are compared. The calculations include the contributions from the intermediate $1s2s2\ell n\ell'$ ($2 \leq n \leq 12$) states. The total DR resonant strength converges quickly as a function of principle quantum number n along the $2\ell n\ell'$ Rydberg series. There are seven distinct peaks in the energy range $26 \leq E \leq 46$ GeV of the projectile. The first three peaks can be identified as $1s2s^22p_{1/2}$ + $1s2s2p^2_{1/2}$, $1s2s^22p_{3/2}$ + $1s2s2p_{1/2}\,2p_{3/2}$ and $1s2s2p^2_{3/2}$. The last four peaks arise from $1s2s2\ell3\ell'$, $1s2s2\ell4\ell'$, $1s2s2\ell n\ell'$($n \geq 5$), and $1s2s3\ell3\ell'$ configurations, respectively. Including Breit interaction in calculations of Auger rates can be seen to have significant influence on most of the peak heights except peak B (e.g. peak A is increased by a factor of 2). Similar calculations were also performed for U^{90+} in collisions with H_2 for the intermediate K-LL and K-LM states (Fig. 2). The same relativistic effects seen for U^{89+} can be applied to the case of U^{90+}.

In Fig. 3, the experimental RTEX cross sections for U^{90+} in collisions with H_2 [8] are compared with the present theoretical results from the MCDF model including the contributions from the $1s2\ell n\ell'$ ($2 \leq n \leq 12$) states. Excellent agreement between theory and experiment both in peak positions as well as peak amplitudes has been attained. Recently, Pindzola and Badnell [15] have also calculated the RTEX cross sections for U^{q+} (q = 89 and 90) in H_2 using the MCDF method and obtained theoretical results which are in good agreement with our MCDF predictions [13].

Similar MCDF calculations have been extended to U^{82+} + H_2 system in order to study the effects of relativity on the RTEX cross sections involving L-shell excitation. The theoretical results are displayed in Fig. 4. In nonrelativistic LS coupling approximation, the RTEX cross section for the L-MM transitions shows one strong peak at 1.7 GeV while, in the relativistic intermediate coupling case, there are five additional small peaks spreading from 0.2 GeV to 4.0 GeV. This is due to the fact that the relativistic effects and spin-orbit interaction widen the L-MM Auger spectra from 3.15-4.47 KeV to 0.645-8.85 KeV. Furthermore, the main peak is shifted to slightly higher energy and is reduced by more than a factor of 2 in its amplitude. The total DR strength from the L-MM transitions is reduced by 27% due to the effects of relativity. The reduction is mainly caused by the changes in energies and wave functions. Although a few strong L-MM Auger lines have been changed by more than 50% due to the inclusion of the Breit interaction in calculations of Auger matrix elements, the RTEX cross sections show little change because of the smearing in the convolution procedure (Fig. 4).

The RTEX cross sections for U^{q+} (q = 82, 89 and 90) in collisions with helium and carbon targets have also been calculated in impulse approximation using the MCDF method. Similar relativistic effects have been found for these cases. Some of the results have been reported in Ref. 13.

IV. CONCLUSIONS

Effects of relativity have been found to have significant impact on the calculations of the RTEX cross sections arising from k-shell excitation of heavy ion in collisions with light targets. Relativistic effects not only shift the peak positions but also change the number of peaks. It is essential to include the Breit interaction in calculations of Auger matrix elements. The total DR strengths for U^{89+} and U^{90+} are increased by 50% because of the inclusion of the relativistic effects. For cases involving L-shell excitation, effects of relativity on RTEX cross sections manifest themself mainly through the spin-orbit interaction. Inclusion of Breit interaction in calculations of Auger rates has no effect on the L-shell RTEX cross sections. For U^{82+}, the total L-MM DR strength is reduced by 27% due to the effects of relativity.

ACKNOWLEDGMENTS

The author would like to thank W. Graham and M. Clark for making their experimental data available before publication. This work was performed under the auspices of the U.S. Department of Energy by the Lawrence Livermore National Laboratory under Contract No. W-7405-ENG-48.

REFERENCES

[1] D. Brandt, Phys. Rev. A 27, 1314 (1983).

[2] J. A. Tanis, S. M. Shafroth, J. E. Willis, M. Clark, J. Swenson, E. N. Strait, and J. R. Mowat, Phys. Rev. Lett. 47, 828 (1981).

[3] J. A. Tanis, E. M. Berstein, W. G. Graham, M. Clark, S. M. Shafroth, B. M. Johnson, K. W. Jones, and M. Meron, Phys. Rev. Lett. 49, 1325 (1982).

[4] J. A. Tanis, E. M. Berstein, M. P. Stockli, M. Clark, R. H. McFarland, T. J. Morgan, K. H. Berkner, A. Schlacter, and J. W. Stearns, Phys. Rev. Lett. 53, 2551 (1984).

[5] J. A. Tanis, E. M. Berstein, M. W. Clark, W. G. Graham, R. H. McFarland, T. J. Morgan, J. R. Mowat, D. W. Mueller, A. Muller, M. P. Stockli, K. H. Berkner, P. Gohil, R. J. McDonald, A. S. Schlacter, and J. W. Stearns, Phys. Rev. A 34, 2543 (1986).

[6] M. Schulz, R. Schuch, S. Datz, E. L. B. Justiniano, P. D. Miller, and H. Schöne, Phys. Rev. A 38, 5454 (1988).

[7] W. G. Graham et al., in Proceedings of the Sixteenth International Conference on the Physics of Electronic and Atomic Collisions, New York, 1989, Abstracts of Contributed Papers, edited by A. Dalgarno et al. (XVI ICPEAL Program Committee, New York, 1989).

[8] W. G. Graham, K. H. Berkner, E. M. Bernstein, M. W. Clark, B. Feinberg, M. A. McMahan, T. J. Morgan, W. Rathbun, A. S. Schlachter and J. A. Tanis, submitted to Phys. Rev. Lett.

[9] J. M. Feagin, J. S. Briggs, and T. M. Reeves, J. Phys. B 17, 1057 (1984).

[10] D. J. McLaughlin and Y. Hahn, Phys. Lett. 112 A, 389 (1985); Phys. Rev. A 37, 3587 (1988).

[11] C. P. Bhalla and K. R. Karim, Phys. Rev. A 39, 6060 (1989).

[12] N. R. Badnell, Phys. Rev. A 40, 3579 (1989); ibid 42, 209 (1990).

[13] M. H. Chen, Phys. Rev. A 41, 4102 (1990).

[14] M. H. Chen, Phys. Rev. A (in press).

[15] M. S. Pindzola and N. R. Badnell, Phys. Rev. A xx, xxx (1990).

[16] Y. Hahn, Phys. Rev. A 40, 2950 (1989).

[17] I. P. Grant, B. J. McKenzie, P. H. Norrington, D. F. Mayers, and N. C. Pyper, Comput. Phys. Commun. 21, 207 (1980).

[18] M. H. Chen, Phys. Rev. A 31, 1449 (1985).

[19] M. J. Seaton and P. J. Storey, in Atomic Processes and Applications, edited by P. G. Burke and B. L. Moisewitsch (North-Holland, Amsterdam, 1976), p. 133.

[20] J. B. Mann and W. R. Johnson, Phys. Rev. A 4, 41 (1971).

[21] B. J. McKenzie, I. P. Grant and P. H. Norrington, Comput. Phys. Commun. 21, 233 (1980).

[22] J. S. Lee, Chem. Phys. 60, 4906 (1977).

[23] F. Biggs, L. B. Mendelsohn, and J. B. Mann, At. Data Nucl. Data Tables 16, 201 (1975).

[24] M. H. Chen, in Atomic Inner-Shell Physics, edited by B. Crasemann (Plenum, New York, 1985); Nucl. Instr. and Meth. B 43, 366 (1989).

FIGURE CAPTIONS

Fig. 1 RTEX cross sections for the $U^{89+} + H_2$ collisions as functions of projectile energy. The solid curve displays the MCDF predictions including the contributions from the generalized Breit operator. The dashed curve represents the results from the MCDF method without including Breit interaction in calculations of Auger rates. The intermediate states contributing to the peaks are A, $1s2s^22p_{1/2} + 1s2s2p^2_{1/2}$; B, $1s2s^22p_{3/2} + 1s2s2p_{1/2}2p_{3/2}$; C, $1s2s2p^2_{3/2}$; D, $1s2s2\ell3\ell'$; E, $1s2s2\ell4\ell'$; F, $1s2s2\ell n\ell'$ ($n \geq 5$); and G, $1s2s3\ell3\ell'$. From Ref. 13.

Fig. 2 RTEX cross sections from the K-LL and K-LM transitions for the $U^{90+} + H_2$ collisions as functions of projectile energy. The legend is the same as in Fig. 1.

Fig. 3 Present theoretical RTEX cross sections for the $U^{90+} + H_2$ collisions including contributions from the $1s2\ell n\ell'$ ($2 \leq n \leq 12$) states are compared with experiment (Ref. 8).

Fig. 4 RTEX cross sections from the L-MM transitions for the $U^{82+} + H_2$ collisions as functions of projectile energy. The solid curve shows the MCDF results including the contributions from the transverse Breit interaction. The dotted curve displays the values without including Breit interaction in calculations of Auger rates. The dashed curve represents the results from the nonrelativistic LS coupling calculations.

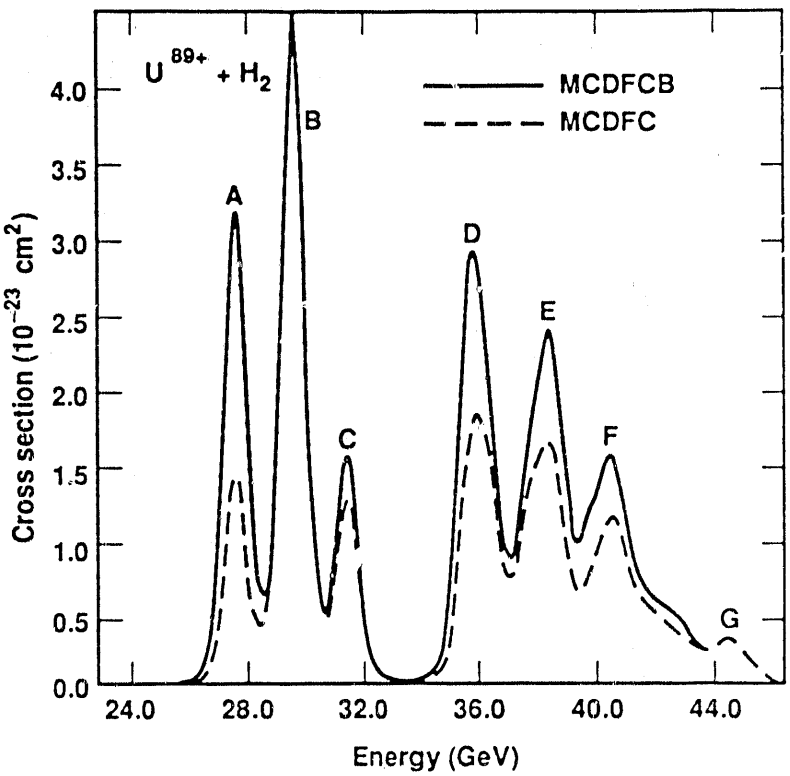

U 89+ + H2
MCDFCB
MCDFC
A
B
C
D
E
F
G
Cross section (10^-23 cm^2)
4.0
3.5
3.0
2.5
2.0
1.5
1.0
0.5
0.0
24.0
28.0
32.0
36.0
40.0
44.0
Energy (GeV)

Fig. 1

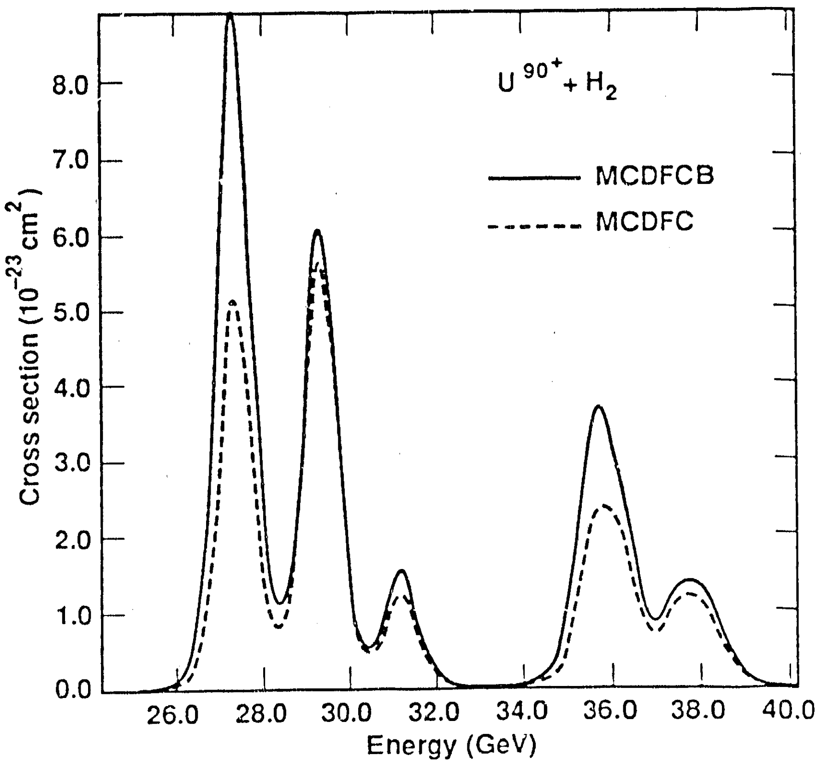
U $^{90+}$ + H_2
MCDFCB
MCDFC
Cross section (10^{-23} cm^2)
Energy (GeV)
0.0
1.0
2.0
3.0
4.0
5.0
6.0
7.0
8.0
26.0
28.0
30.0
32.0
34.0
36.0
38.0
40.0

Fig. 2

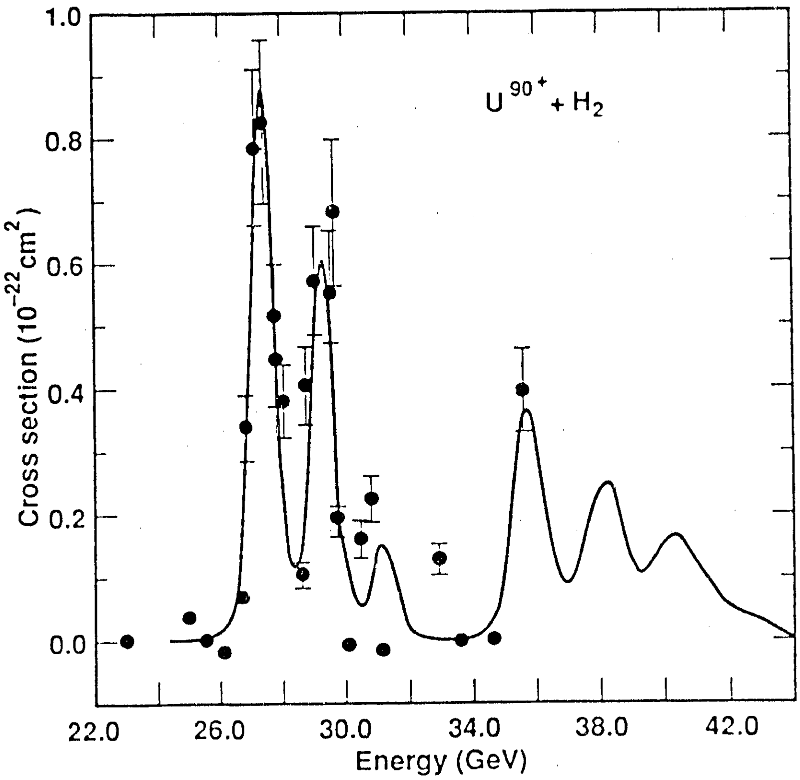
1.0
0.8
0.6
0.4
0.2
0.0
Cross section ($10^{-22}cm^2$)
$U^{90+} + H_2$
22.0
26.0
30.0
34.0
38.0
42.0
Energy (GeV)

Fig. 3

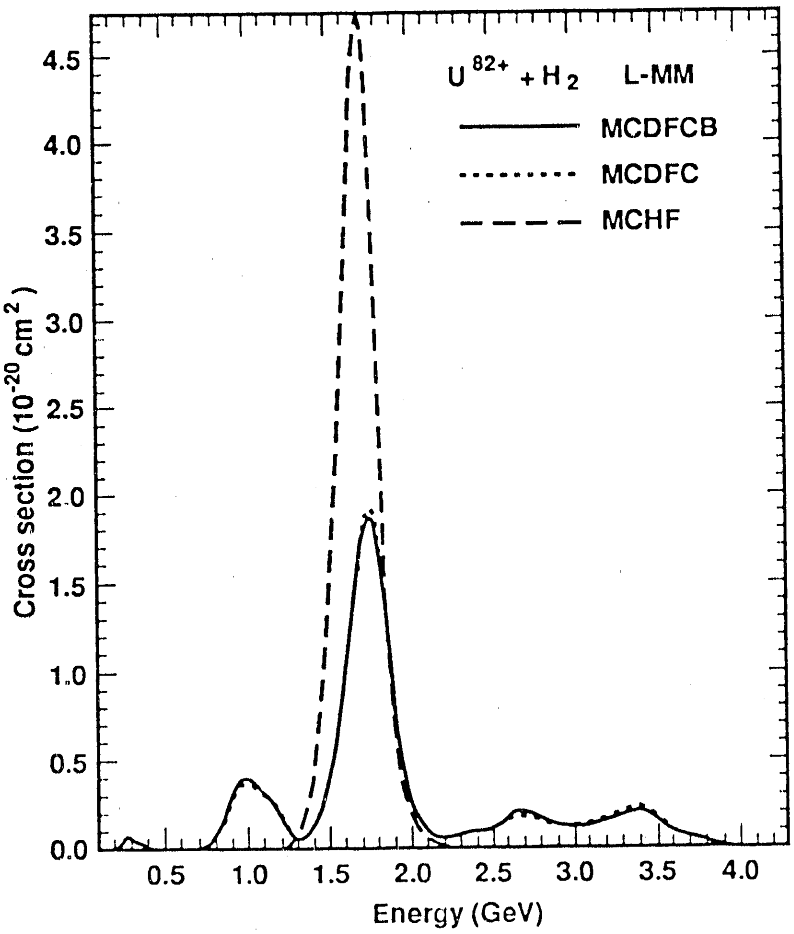

U 82+ + H 2 L-MM
MCDFCB
MCDFC
MCHF
4.5
4.0
3.5
3.0
2.5
2.0
1.5
1.0
0.5
0.0
Cross section (10-20 cm 2)
0.5
1.0
1.5
2.0
2.5
3.0
3.5
4.0
Energy (GeV)

Fig. 4

END

DATE FILMED

02 / 20 / 91